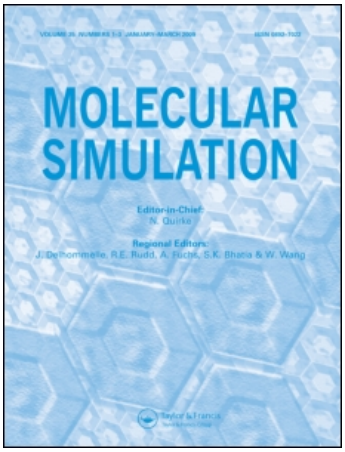

Molecular Simulation
Publication details, including instructions for authors and subscription information:
http://www.informaworld.com/smpp/title~content=t713644482

Computation of densities, bulk moduli and glass transition temperatures of vinylic polymers from atomistic simulation

N. Metatla[a]; A. Soldera[a]
[a] Department of Chemistry, Université de Sherbrooke, Sherbrooke, Qué., Canada

To cite this Article Metatla, N. and Soldera, A.(2006) 'Computation of densities, bulk moduli and glass transition temperatures of vinylic polymers from atomistic simulation', Molecular Simulation, 32: 14, 1187 — 1193
To link to this Article: DOI: 10.1080/08927020601059901
URL: http://dx.doi.org/10.1080/08927020601059901

Molecular Simulation, Vol. 32, No. 14, 15 December 2006, 1187–1193

Taylor & Francis
Taylor & Francis Group

Computation of densities, bulk moduli and glass transition temperatures of vinylic polymers from atomistic simulation

N. METATLA and A. SOLDERA*

Department of Chemistry, Université de Sherbrooke, Sherbrooke, Qué., Canada J1K 2R1

(Received September 2006; in final form October 2006)

The aim of molecular modeling is to mimic reality by considering approximations appropriate to the scale at which the simulation is carried out. At the atomic level, forcefields that represent average atomic interactions are used. However, the phase space has to be adequately explored in order to compare successfully computed and experimental properties. The procedure exposed in this article considers an initial selection of relevant configurations on which a simulated annealing process is applied using the first generation forcefield OPLS, followed by a uniform hydrostatic compression using the second generation forcefield COMPASS©. The resulting data are fitted by an equation of state, from which density and bulk modulus are determined. The glass transition is then simulated and T_gs are computed. Our approach is tested using a series of vinylic polymers, which differ from each other by small variations in atomic interaction combinations. The excellent agreement with experimental data shows the validity of the procedure exposed. Moreover, a clear linear relationship between simulated and experimental T_gs is revealed.

Keywords: Equation of state; Simulated annealing; Tacticity; Molecular dynamics

1. Introduction

Using molecular dynamics (MD) simulations with a full description of the atomic interactions through the use of forcefield, involves an integration step of 10^{-15} s to remain on the surface of potential energy [1]. Short simulation durations can thus only be accessed and obtaining relaxed polymer systems was evidently called into question [2]. Atomistic MD simulations inspect the portion of phase space that is directly located near the initial location [3]. The phase space is actually split into two spaces, the configurational and the momentum spaces, both of $3N$ dimension, with N the number of atoms in the system [4]. Accordingly, generation of the initial configurations is of major importance since they dictate the final properties [3,5]. Great efforts have thus been carried out during the last decade to generate accurate amorphous initial configurations. The original breakthrough has been done by Theodorou and Suter [3] who proposed a polymer chain generation procedure based on a modified RIS model to include long range excluded volume, followed by a series of energy optimization (relaxation and minimization). This procedure is implemented in the Amorphous_Cell© code from Accelrys. Different methods to generate polymer chains have been proposed since then using phantom chain growth, coarse-grained guesses or advanced Monte Carlo algorithms [6–13]. However, the purpose of this study is not to compare the different methods, but rather to use an existing one, implemented in the Amorphous_Cell© code and attempt to circumvent some of its drawbacks. One of the major drawbacks is actually in generating relaxed configurations of a long chain [10,14].

The proposed procedure to get optimized configurations could not ascertain that relaxed structures have been obtained since the simulation times that have been used are low compared to the polymer relaxation times. However it yields compounds whose density and bulk modulus are in good agreement with experimental data and whose computed T_gs are clearly reproducible. In order to confirm the accuracy of the procedure, it has been applied to five polymers. These polymers are vinylic polymers, which differ from each other by small variations in atomic interaction combinations. Atomistic simulations of such polymers are therefore important since it can deal with these slight variations at the atomic scale. These

*Corresponding author. Email: armand.soldera@usherbrooke.ca

Molecular Simulation
ISSN 0892-7022 print/ISSN 1029-0435 online © 2006 Taylor & Francis
http://www.tandf.co.uk/journals
DOI: 10.1080/08927020601059901

polymers are: polyethylene (PE), isotactic and syndiotatic poly (methyl methacrylate) (i-PMMA and s-PMMA), isotactic and syndiotactic poly (α-methyl styrene) (i-PαMS and s-PαMS), polymethylacrylate (PMA) and polystyrene (PS). Except for PE, they all possess a side-chain: an ester group for PMA and PMMA and a phenyl group for PS and PαMS. The presence of an additional α-methyl group in PMMA and PαMS imparts to these polymers different T_gs according to the tacticity of their chain [15], while no significant difference in T_gs is observed between stereomers of PMA and PS. Both chain tacticities of these latter polymers have also been simulated.

It has to be pointed out that an extensive equilibrium procedure based on a series of MD simulations has been proposed by Hoffmann *et al.* [16–18] using the Amorphous_Cell© code. Despite the excellent agreement between simulated and experimental densities, it is central process unit (CPU) time demanding. An alternative approach is exposed in this text to get systems with accurate density values. The proposed approach consists in a simulated annealing process followed by a uniform hydrostatic compression procedure. The uniform hydrostatic compression is usually applied to inorganic compounds to attain their crystal structure [19]. The crystallographic parameter, the cell edge for a cube, is varied until a minimum in energy is reached. The curve of energy with respect to the volume is then fitted with an equation of states (EOS) [20]. Density and bulk modulus can then be extracted. Moreover, a combination of first and second-generation forcefields is used in a complementary fashion in order to gain in computer time resources. T_gs can thus be computed and compared to experimental data.

2. Molecular modeling procedure

Each polymer chain considered in this study possesses 100 repeat units (RUs). The Amorphous_Cell© code, based on the self-avoiding walk procedure [21], is used to generate the polymer chain imbedded in a cell with periodic boundary conditions. The procedure is based on the knowledge of the conditional probability to increment RUs during the chain generation. It is actually determined by the calculation of the long-range non-bond energy considering atoms that are separated by more than two bonds [22]. The consideration of only short-range interactions through the pentane effect, was not sufficient to homogeneously fill the entire cell [3]. However, the modification of this conditional probability to explicitly consider long-range interactions, has direct consequences on the percentage of rotameric states and consequently on the values of the end-to-end distance and the radius of gyration. It is thus proposed to initially generate 50 configurations. About 10 configurations are then selected according to two criteria. The first criterion consists of the selection of the apposite portion of the configurational space by comparing simulated and experimental end-to-end distances in order to reduce considerably the standard mean deviation. The purpose for this selection is to get configurations that better mimic reality and thus it tends to circumvent some of the drawbacks of the chain generation: atomistic simulation and experience are carried out in a complementary fashion. The second criterion is purely energetic: configurations of lower energy are selected. To confirm the correct selection of the final configurations, percentages of rotameric states have been calculated and reported in table 1. They are compared to values stemming from the RIS matrix of statistical weights computed for a bond in the middle of the chain. Due to the introduction of long-range interactions, a slight difference is observed. It has to be noted that only three rotameric states have been considered for the calculations of the rotameric percentages. However, the six rotameric states of both PMMA have been clearly revealed, as it is shown for instance for one configuration of s-PMMA at 300 K in figure 1 [23].

Table 1. Simulated and computed RIS (in parentheses) percentages for studied polymers.

	Simulation (RIS model)		
Polymer	*t* %	*g* %	$\bar{g}$ %
PE[†]	55 ± 3 (60)	23 ± 4 (20)	22 ± 4 (20)
i-PMA[‡]	60 ± 4 (67)	20 ± 4 (22)	20 ± 3 (11)
s-PMA[‡]	71 ± 7 (93)	12 ± 5 (4)	17 ± 5 (3)
i-PMMA[¶]	61 ± 5 (72)	21 ± 6 (20)	18 ± 4 (8)
s-PMMA[¶]	72 ± 3 (88)	14 ± 2 (4)	14 ± 3 (8)
i-PS[§]	43 ± 5 (52)	48 ± 6 (47)	9 ± 4 (1)
s-PS[§]	67 ± 4 (80)	26 ± 5 (19)	7 ± 3 (1)
i-PαMS[‖]	74 ± 4 (84)	14 ± 3 (8)	12 ± 3 (8)
s-PαMS[‖]	83 ± 5 (94)	8 ± 3 (3)	9 ± 2 (3)

[†] Jernigan, R. L.: Flory, P. J. J. Chem. Phys. 1969; 50:4165.
[‡] Ojalvo, E. A.; Saiz, E.; Masegosa, R. M.; Harnández-Fuentes, I. Macromolecules 1979; 12:865.
[¶] Vacatello, M.; Flory P. J. Macromolecules 1986; 19:405.
[§] Biskup, U.; cantow H. J. Makromol. Chem. 1973; 168:315.
[‖] Sundararajan, P. R. Macromolecules 1977; 10:623.

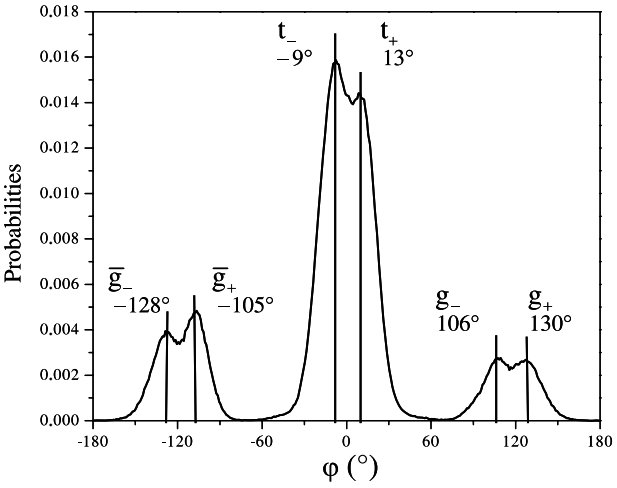

Figure 1. Computed probabilities of backbone dihedral angles of s-PMMA at 300 K. The Vacatello and Flory's notation is used to design rotameric states.

2.1 Simulated annealing process

The simulated annealing process requires an important demand in calculation due to the great number of polymer chain configurations involved during the simulations (90 polymers, number that considers both tacticities of PS and PMA) and the long duration of the entire MD simulations. A first generation forcefield, OPLS, was then chosen for those simulations.

This relaxation step is performed on a cluster of processors in parallel employing the DL_POLY code [24] with the Verlet-leapfrog integration algorithm using a 1 fs integration time step [25]. The NPT ensemble, i.e. constant number of particles, pressure and temperature, was used during the simulated annealing process. To keep the system at prescribed temperature and pressure the Berendsen thermostat and barostat were employed [26]. The cut-off of the non-bonded interactions has been done using the Ewald summation method [27]. The relaxation begins with a heating of the system from 300 to 800 K. The system is thereafter cooled from 800 to 240 K using a cooling rate of 1.2×10^{13} K/min. A relatively slower cooling rate of 1.2×10^{12} K/min has also been used for both PMMA chain tacticities. The final temperature corresponds to the glassy state for all the studied polymers. It has to be pointed out that this procedure is similar to the simulated dilatometry [28]. However, the T_gs are not reported at this point since non reproducible values have been obtained. A specific optimization procedure has thus been undertaken and is exposed in the following paragraph.

2.2 Uniform hydrostatic compression

To determine the crystal structure of some inorganic compounds, a uniform hydrostatic compression is employed [19]. The computed energy is reported with respect to the cell parameter, or to the cell volume. The crystal structure corresponds to the configuration of minimum energy. The set of data is usually fitted by an EOS, which allows the determination of density and bulk modulus. This procedure was applied to the polymer configurations after the simulated annealing has been applied. In fact, compression is initially carried out since the processes of chain generation and relaxation performed in the isotherm–isochore ensemble, exposed in the previous paragraph, involve an expansion of the cell. An example of data stemming from application of uniform hydrostatic compression on five configurations of each chain tacticity of PMMA is displayed in figure 2. As can be observed from figure 2, different compression steps have been reported. Actually the procedure consists into two stages. An initial compression of the cell is carried out uniformly with variation steps of the cell edge of 0.1 Å and an energetic convergence of 10 kcal/mol. When a minimum in energy is reached, the optimization is refined and a step of 0.001 Å is then imposed, with an energetic convergence of 0.1 kcal/mol. It has to be pointed out that

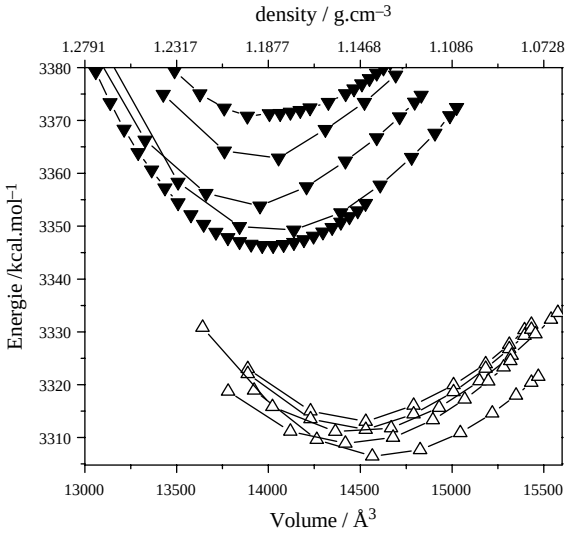

Figure 2. Graph of energy with respect to cell volume during a uniform hydrostatic compression for 5 configurations of i-PMMA (▼) and s-PMMA (Δ).

compression or dilatation could occur to reach this latter minimum since a downhill energy variation is always looking for. The fitting process is done at this stage yielding the values of the density and the bulk modulus.

The forcefield which has been used during this process is COMPASS©, a second generation forcefield, from Accelrys. A comparative study using OPLS has been carried out for both PMMA tacticities, PS and PMA. COMPASS© has been specifically built up to accurately represent non-bond interactions. The use of this forcefield to obtain the minimum in energy is actually not incompatible with the choice of a first generation forcefield to get the polymer in the rubbery phase. The OPLS forcefield has been parameterized in order to better mimic the liquid phase. These two forcefields serve two different goals: energy minimization using COMPASS© and energy relaxation (and T_g determination) employing OPLS.

2.3 Computation of bulk modulus and density

Two ways are used to compute bulk modulus and density. In the first case, the same procedure as used for inorganic compounds is applied. The Murnaghan [29] EOS, equation (1), deriving from continuum mechanics, was chosen to fit the data stemming from the uniform hydrostatic compression. It has to be noted that other EOS could be employed, but differences in the stemming results are not significant in the vitreous state of polymers.

$$E(V) = B_0^{\mathrm{M}} V_0 \left[\frac{1}{B'(B'-1)} \left(\frac{V_0}{V} \right)^{B'-1} + \frac{1}{B'} \frac{V}{V_0} - \frac{1}{B'-1} \right] + E_0 \tag{1}$$

where V_0 is the volume at the minimum energy, directly yielding the density, ρ^{M}; B_0^{M} is the bulk-modulus; and B' is

the pressure derivative at zero pressure; the superscript M refers to the Murnaghan EOS.

The second way to compute the bulk modulus stems from the fact that the system is in the vitreous state and entropic variations are therefore negligible [30]. Consequently, the bulk modulus, or the inverse of the compressibility, $B = -V_o(\partial p/\partial V)_{N,T}|_o$, where p is the pressure imposed to the system, could be rewritten under the following form:

$$B = V_o \left(\frac{\partial^2 E}{\partial V^2} \right)_{N,T} \Bigg|_o \quad (2)$$

the subscript o indicates that the value is obtained for the minimum in energy. Expressing the energy with a quadratic equation, following the Hooke's law, directly yields the values of B and density, ρ. The computed values and their standard-mean deviation, are reported for each polymer in tables 2 and 3 and compared to experimental data.

2.4 Simulated dilatometry

Experimentally the dilatometric technique is currently employed to determine the T_g. As the system cools down, the specific volume, i.e. the inverse density, is reported for different temperatures. The departure from a linear relationship between the specific volume and the temperature yields the value of the T_g which corresponds to the transition from the rubbery to the vitreous phases. To apply this procedure to our systems, optimized configurations stemming from the uniform hydrostatic compression, have been gently heated to 800 K. Configurations are then kept at this temperature during 100 ps in the *NVT* ensemble i.e. constant number of particles, volume and temperature. Thereafter, the system is cooling down to 240 K by 20 K steps of 100 ps duration each, giving a cooling rate of 1.2×10^{13} K/min. During this process to get the T_gs, the first generation OPLS forcefield is used. In this forcefield, the bonding potential parameter terms come from the AMBER forcefield, while the non-bond parameters result from the use of the BOSS code [31,32]. These latter parameters are specifically computed to accurately mimic the liquid phase. A better determination of T_gs is obtained using OPLS comparatively to the use of AMBER whose non-bond parameters have been determined from crystal structures: difference in T_gs between the two configurations of PMMA has been shown to be better depicted using OPLS [33,34].

Table 2. Simulated bulk moduli obtained using COMPASS© and OPLS forcefields, compared to experimental data for studied polymers. See text for more details.

	Simulated B (GPa)		
Polymer	*COMPASS©*	*OPLS*	*Experimental B (GPa)*
PE	5.0 ± 0.5		4.70[†]
PMA	6.2 ± 0.8		
i-PMMA	6.6 ± 0.5	4.9 ± 1.3	5.93[‡]
	(6.4 ± 0.4)	(5.0 ± 1.0)	5.77[¶]
s-PMMA	5.4 ± 0.4	4.9 ± 1.3	
	(5.1 ± 0.4)	(4.8 ± 1.1)	
PS	5.6 ± 0.6	5.3 ± 0.5	6.0[†]
			4.5[§]
i-PαMS	5.2 ± 0.9		
s-PαMS	4.4 ± 0.7		

[†] Bridgman, P. W. Proc. Am. Acad. Arts Sci. 1948;76;71.
[‡] Weishaupt, K.; Krbecek, H.; Peitralla, M.; Hochheimer, H. D.; Mayr, P. Polymer 1995;36;3267.
[¶] Hartmann, B. In *Physical Properties of Polymers Handbook*; Mark, J.E.,Ed.; A.I.P.:Woodbury, NY, 1996; Vol. Ch 49 pp 667.
[§] Plazek, D. J.; Ngai, K. L. In *Physical Properties of Polymers Handbook*; Mark, J. E., Ed.; A.I.P.: Woodbury, NY, 1996: Vol. Ch 12, pp 139.

Table 3. Simulated densities obtained using COMPASS© and OPLS forcefields, compared to experimental data for studied polymers. See text for more details.

	Simulated ρ (g cm^{-3})		
Polymer	*COMPASS©*	*OPLS*	*Experimental ρ (g cm^{-3})*
PE	0.900 ± 0.009		0.86[†]
PMA	1.245 ± 0.012	1.159 ± 0.019	1.222[‡]
i-PMMA	1.192 ± 0.005	1.141 ± 0.014	1.22[‡]
	(1.189 ± 0.003)	(1.139 ± 0.012)	
s-PMMA	1.157 ± 0.006	1.108 ± 0.010	1.19[‡]
	(1.155 ± 0.004)	(1.105 ± 0.011)	
PS	1.073 ± 0.010	1.067 ± 0.007	1.062[¶]
			1.075[§]
i-PαMS	1.057 ± 0.014		1.073[‖]
s-PαMS	1.032 ± 0.019		1.073[‖]

[†] Alger, M. Polymer Science Dictionary: Chapman & Hall, 1997.
[‡] Ellis, B. Polymers—a property database. Sheffield: Chapman & Hall, 2000.
[¶] Mosiewicki, M.; Borrajo, J; Aranguren, M. I. Polym. Int. 2005;54:829.
[§] Naumann, M.; Duran, R. Polym. Perprints, A.C.S. 1991;32:96.
[‖] Cowie, J. M. G.; Toporowski, P. M. J. Macromol. Sci. Phys. 1969;B3:81.

3. Results and discussion

Despite the use of a relaxation process, the end-to-end distance does not greatly vary with temperature from its initial value as it is shown for the two tacticities of PMMA in figure 3. These small variations clearly reveal that

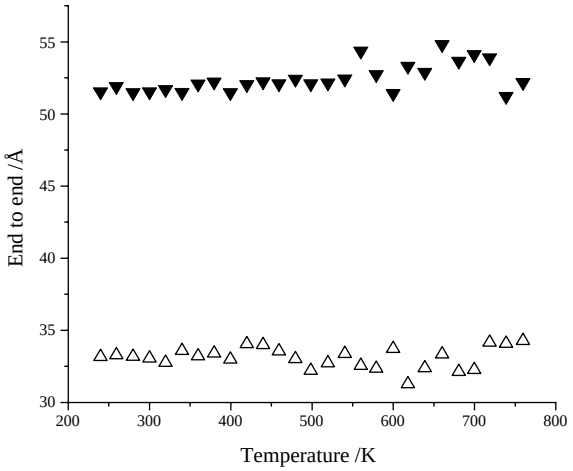

Figure 3. End-to-end distance with respect to the temperature for i-PMMA (▼) and s-PMMA (Δ), during a simulated annealing process.

a limited exploration of the configurational space has been made and thus show the importance to appropriately select several initial configurations to get relziable averages. After the simulated annealing has been performed on these configurations, the T_gs could be obtained and conclusions regarding to the difference in the T_gs between the two stereomers, could be extracted [35,36]. However an analysis of the glass transition involving several polymers could not be accurately performed since non-reproducible T_gs have been obtained. Nevertheless, this relaxation process is important to get final structures on which uniform hydrostatic compression is carried out.

Applying uniform hydrostatic compression (or dilatation) to the vitreous state of polymers involves configurational changes. As a typical example, energy and end-to-end distance with respect to the volume are reported in the same graph in figure 4, for one configuration of s-PMA. In this case, a refine dilatation has been performed on the configuration of minimum energy obtained during the first stage described in Section 2.2. Different regions are defined according to the jumps in the energy curve, as displayed in figure 4. In each region, the end-to-end distance increases with volume and the percentage of *trans* state remains constant as shown in table 4. The change in the end-to-end distance, or in the radius of gyration, during hydrostatic variation, is not significant when all the configurations of polymers are considered since it is included in the standard mean deviation.

For each region displayed in the graph of figure 4, data have been fitted using the Murnaghan EOS, equation (1) and a quadratic equation, thus yielding values for the bulk modulus and the density. These fitting values are reported in table 4. In Region 3, the derivative of energy is zero, but it does not correspond to the minimum in energy since there is a jump to lower energy at higher dilatation, corresponding to Region 4. From the minimum in energy in this Region 4, a compression has been carried out giving Region 5 for which computed bulk modulus and density are reported in table 4. For sake of clarity in figure 4, the end-to-end distance of Region 5 is not reported. Regions 3

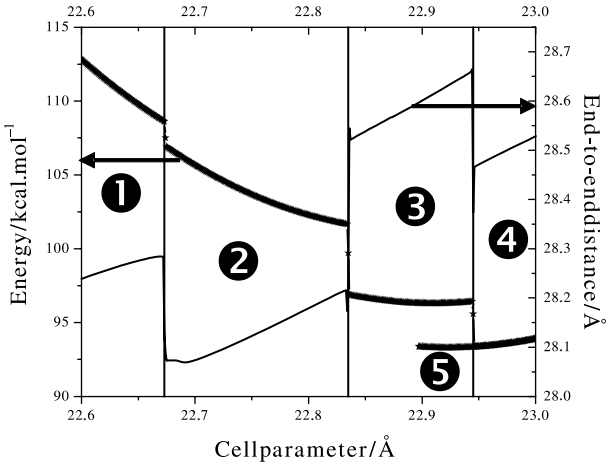

Figure 4. Energy (★) and end-to-end distance (—) variation with respect to the cell parameter for one configuration of s-PMA.

Table 4. Comparison between bulk modulus and density values computed using equations (1) and (2), for the different regions defined on figure 4.

		Murnaghan EOS		*Quadratic equation*	
Region	*Percentage of t*	ρ^M (g cm^{-3})	B_0^M (GPa)	ρ (g cm^{-3})	B (GPa)
1	63%	1.1917	5.31	1.2054	11.7
2	64%	1.1908	7.29	1.1922	8.34
3	63%	1.1891	7.19	1.1891	7.18
4	64%	1.1869	7.26	1.1878	6.00
5	64%	1.1871	7.16	1.1871	7.18

and 5 both exhibit an energy derivative of zero, but a different minimum in energy. However the fits yield comparable values of bulk modulus and density. As soon as a region does not exhibit the zero energy derivative, the two fitting equations give different results. The departure from the data obtained at the equilibrium structure is more pronounced for the quadratic equation since the Hooke's law becomes less relevant. Accordingly density and bulk modulus have to be computed at the equilibrium position.

For both PMMA tacticities, PMA and PS, the two forcefields, OPLS and COMPASS© have been used during the hydrostatic uniform compression and the resulting data are reported in tables 2 and 3. From table 3, density values obtained using COMPASS© show an excellent agreement with experimental data. The non-bonding interactions in COMPASS© has been greatly improved comparatively to *pcff* [37,38], resulting in a better representation of densities. In the case of density values computed using the OPLS forcefield, the agreement is excellent for PS, while for PMMA and PMA, the resulting values are slightly lower than experimental data. An important aspect to be considered is that the difference in the densities between PMMA stereomers is accurately reproduced whatever forcefield is employed.

Difference between both PMMA configurations is also observable for the bulk modulus computed using COMPASS© thus revealing that bulk modulus depends on the chain tacticity. No experimental data has been found in the literature to confirm this finding. Furthermore, the same value is obtained when OPLS is considered. However, the simulated values for both forcefields are in same order than experimental data. Concerning PS, computed values are found in the same range than the different experimental bulk moduli found in the literature. Actually no further conclusions could be extracted from the simulation of bulk modulus due to the lack of experimental data. Nevertheless, as for PMMA, PαMS exhibits bulk modulus and density values that depend on the tacticity of the chain [15].

The dependence of bulk moduli and densities on the cooling rates during the simulated annealing process has also been regarded. For both PMMA configurations, two cooling rates have thus been used. Uniform hydrostatic compression was applied to the final structure and bulk modulus and density were then computed. Results are

Table 5. Simulated T_gs compared to experimental data for studied polymers.

Polymer	*Simulated T_g (K)*	*Experimental T_g (K)*
PE	327 ± 3	194
PMA	406 ± 4	280[†]
i-PMMA	445 ± 6	318[‡]
s-PMMA	513 ± 7	387[‡]
PS	484 ± 5	362[¶]
i-PαMS	508 ± 6	390[§]
s-PαMS	588 ± 6	

[†] Lu and B. Jiang, Polymer **32**, 471 (1991).
[‡] K. Ute, N. Miyatake, and K. Hatada, Polymer **36**, 1415 (1995).
[¶] L. H. Sperling, *Introduction to Physical Polymer Science* (John Wiley & Sons, Ins., New York, 1992).
[§] L. Malhotra, L. Minh, and L. P. Blanchard, J. Macromol. Sci. Chem. **A12**, 167 (1978).

reported in tables 2 and 3. Values in parentheses reported in these tables correspond to data obtained after a 1.2×10^{12} K/min simulated annealing cooling rate was applied. No dependence on the cooling rates for both properties is observed whatever forcefield is used.

An excellent agreement between experimental and simulated results is thus obtained for all the polymers considered in this work. It has thus been argued that despite the low duration that reported simulations have accessed, simulated dilatometry could be applied to compute T_gs. In table 5 are reported T_g values for the different polymers. Experimental data have been extracted from the Fox–Flory equation. It has to be pointed out that reported values are reproducible. Moreover, despite the great difference with experimental data, a linear relationship is clearly revealed between the simulated and experimental T_gs as can be shown in figure 5. The fitting equation is displayed in equation (3).

$$T_{g\,(\text{simulated})} = 0.96.T_{g\,(\text{experimental})} + 140\,\text{K} \qquad (3)$$

The reliability factor is 99.8%. The difference of 140 K is attributable to the cooling rate used (1.2×10^{13} K/min). Further analysis on the dependence of this parameter on the cooling rate is the subject of an incoming article.

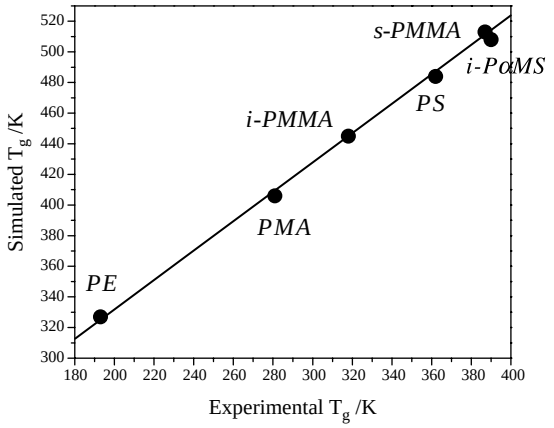

Figure 5. Simulated T_gs of all the studied polymers are reported versus experimental T_gs. The linear fit is also displayed.

4. Conclusion

To by-pass the problem of ergodicity, impossible to solve by atomistic simulation, an appropriate selection of initial configurations based on two criteria, a comparison with experimental data and energetic consideration, is firstly carried out. A simulated annealing is then performed on these configurations. Due to the great demand in computer resources, time and processors, a first generation forcefield, OPLS, specifically designed to address non-bonding interactions in polymers, is used. After this heating-cooling process, the configurations are not in a potential well. A uniform hydrostatic compression is then carried out until a minimum in energy is reached. Due to the lower demand in computer resources, the COMPASS© forcefield is employed. The excellent agreement between ensuing densities and bulk moduli and experimental data suggests that the final configurations can be used to determine reproducible values of T_gs. A very clear relationship between computed and experimental T_gs is thus obtained, confirming the validity of the procedure. A complete analysis of the difference in T_gs with different cooling rates can be undertaken and is the subject of an incoming article.

Acknowledgements

The present work was supported by the Natural Sciences and Engineering Research Council (NSERC) of Canada and Université de Sherbrooke. Computations have been made available thanks to the Canadian Fund Innovation (CFI), the Fonds Québécois de la Recherche sur la Nature et les Technologies (TQRNT) and Réseau Québécoise de Calcul Haute Performance (RQCHP).

References

[1] F. Yonezawa. Computer-simulation methods in the study of noncrystalline materials. *Science*, **260**, 635 (1993).
[2] J. Buchholz, W. Paul, K. Binder. Cooling rate dependence of the glass transition temperature of polymer melts: molecular dynamics study. *J. Chem. Phys.*, **117**, 7364 (2002).
[3] D.N. Theodorou, U.W. Suter. Detailed molecular structure of a vinyl polymer glass. *Macromolecules*, **18**, 1467 (1985).
[4] F. Reif. *Fundamentals of Statistical and Thermal Physics*, McGraw Hill, Boston (1965).
[5] D.J. Tildesley. Molecular simulation: a view from the bond. *Faraday Discuss.*, **100**, C29 (1995).
[6] J.I. McKechnie, D. Brown, J.H.R. Clarke. Methods of generating dense relaxed amorphous polymer samples for use in dynamic simulations. *Macromolecules*, **25**, 1562 (1992).
[7] R. Khare, M.E. Paulaitis, S.R. Lusti. Generation of glass structures for molecular simulations of polymers containing large monomer units: application to polystyrene. *Macromolecules*, **26**, 7203 (1993).
[8] D. Brown, J.H.R. Clarke, M. Okuda, T.J. Yamazaki. The preparation of polymer melt samples for computer simulation studies. *J. Chem. Phys.*, **100**, 6011 (1994).
[9] M. Kotelyanskii, N.J. Wagner, M.E. Paulaitis. Building large amorphous polymer structures: atomistic simulation of glassy polystyrene. *Macromolecules*, **29**, 8497 (1996).
[10] V.G. Mavrantzas, T.D. Boone, E. Zervopoulou, D.N. Theodorou. End-bridging Monte Carlo: a fast algorithm for atomistic simulation

of condensed phases of long polymer chains. *Macromolecules*, **32**, 5072 (1999).
[11] T.C. Clancy, W.L. Mattice. Rotational isomeric state chains on a high coordination lattice: dynamic Monte Carlo algorithm details. *J. Chem. Phys.*, **112**, 10049 (2000).
[12] A. Uhlherr, V.G. Mavrantzas, M. Doxastakis, D.N. Theodorou. Directed bridging methods for fast atomistic Monte Carlo simulations of bulk polymers. *Macromolecules*, **34**, 8554 (2001).
[13] D. Curco, C. Alema. Simulation of dense amorphous polymers by generating representative atomistic models. *J. Chem. Phys.*, **119**, 2915 (2003).
[14] D.S. Pearson, L.J. Fetters, W.W. Graessley, G.V. Strate, E.V. Meerwall. Viscosity and self-diffusion coefficient of hydrogenated polybutadiene. *Macromolecules*, **27**, 711 (1994).
[15] F.E. Karasz, W.J. MacKnight. The influence of stereoregularity on the glass transition temperatures of vinyl polymers. *Macromolecules*, **1**, 537 (1968).
[16] D. Hofman, L. Fritz, J. Ulbrich, C. Schepers, M. Bohning. Detailed-atomistic molecular modeling of small molecule diffusion and solution processes in polymeric membrane materials. *Macromol. Theory Simul.*, **9**, 293 (2000).
[17] D. Hofmann, L. Fritz, J. Ulbrich, D. Paul. Molecular simulation of small molecule diffusion and solution in dense amorphous polysiloxanes and polyimide. *Comput. Theor. Polym. Sci.*, **10**, 419 (2000).
[18] E. Toccia, D. Hofmann, D. Paul, N. Russo, E. Driolia. A molecular simulation study on gas diffusion in a dense poly(ether-ether-ketone) membrane. *Polymer*, **42**, 521 (2001).
[19] R. Dronskowski. *Computational Chemistry of Solid State Materials*, Wiley-VCH, Darmstadt (2005).
[20] J. Shanker, S.S. Kushwah, P. Kumar. Equation of state and pressure derivatives of bulk modulus for NaCl crystal. *Physica B*, **239**, 337 (1997).
[21] H. Meirovitch. Computer simulation of self-avoiding walks: testing the scanning method. *J. Chem. Phys.*, **79**, 502 (1983).
[22] Amorphous_Cell, *Materials Studio is available from Accerlys Inc., San Diedo, CA*
[23] M. Vacatello, P.J. Flory. Conformational statistics of poly(methyl methacrylate). *Macromolecules*, **19**, 405 (1986).
[24] W. Smith, T.R. Forrester. DL_POLY 2.14. *J. Mol. Graphics*, **14**, 136 (1996).
[25] J.M. Haile. *Molecular Dynamics Simulation*, John Wiley & Sons, New York (1992).
[26] H.J.C. Berendsen, J.P.M. Postma, W.F. Van Gunsteren, A. DiNola, J.R. Haak. Molecular dynamics with couplin to an external bath. *J. Chem. Phys.*, **81**, 3684 (1984).
[27] M.P. Allen, D.J. Tildesley. *Computer Simulation of Liquids*, Clarendon Press, Oxford (1987).
[28] D. Rigby, R.-J. Roe. MD simulation of polymer liquid and glass. I. Glass transition. *J. Chem. Phys.*, **87**, 7285 (1987).
[29] F.D. Murnaghan. The compressibility of media under extreme pressures. *Proc. Natl. Acad. Sci. USA*, **30**, 244 (1944).
[30] D.N. Theodorou, U.W. Suter. Atomistic modeling of mechanical properties of polymeric glasses. *Macromolecules*, **19**, 139 (1986).
[31] W.L. Jorgensen, D.S. Maxwell, J. Tirado-Rives. Development and testing of the OPLS all-atom force field on conformational energetics and properties of organic liquids. *J. Am. Chem. Soc.*, **118**, 11225 (1996).
[32] W.L. Jorgensen, J. Tirado-Rives. Molecular modeling of organic and biomolecular systems using BOSS and MCPRO *J. Comput. Chem.*, **26**, 1689 (2005).
[33] A. Soldera, N. Metatla. Glass transition phenomena observed in stereoregular PMMAs using molecular modeling. *Composites Part A*, **36**, 521 (2005).
[34] A. Soldera, N. Metatla. Study of the glass transition temperatures of stereoregular PMMAs using different force fields. *Internet Electron. J. Mol. Des.*, **4**, 721 (2005).
[35] A. Soldera, Y. Grohens. Cooperativity in stereoregular PMMAs observed by molecular simulation. *Polymer*, **45**, 1307 (2004).
[36] A. Soldera, Y. Grohens. Local dynamics of stereoregular PMMAs using molecule simulation. *Macromolecules*, **35**, 722 (2002).
[37] H. Sun. COMPASS: an *ab initio* force-field optimized for condensed-phase applications—overview with details on alkane and benzene compounds. *J. Phys. Chem. B*, **102**, 7338 (1998).
[38] B. Eichinger, D. Rigby, J. Stein. Cohesive energies of Ultem and related molecules from simulations. *Polymer*, **43**, 599 (2002).